

This is a repository copy of *Amine-Borane Dehydropolymerization Using Rh-Based Precatalysts : Resting State, Chain Control, and Efficient Polymer Synthesis*.

White Rose Research Online URL for this paper:

<https://eprints.whiterose.ac.uk/162033/>

Version: Published Version

---

**Article:**

Ryan, David E., Andrea, Kori A., Race, James J. et al. (3 more authors) (2020) Amine-Borane Dehydropolymerization Using Rh-Based Precatalysts : Resting State, Chain Control, and Efficient Polymer Synthesis. *ACS Catalysis*. pp. 7443-7448. ISSN 2155-5435

<https://doi.org/10.1021/acscatal.0c02211>

---

**Reuse**

This article is distributed under the terms of the Creative Commons Attribution (CC BY) licence. This licence allows you to distribute, remix, tweak, and build upon the work, even commercially, as long as you credit the authors for the original work. More information and the full terms of the licence here:

<https://creativecommons.org/licenses/>

**Takedown**

If you consider content in White Rose Research Online to be in breach of UK law, please notify us by emailing [eprints@whiterose.ac.uk](mailto:eprints@whiterose.ac.uk) including the URL of the record and the reason for the withdrawal request.

# Amine–Borane Dehydropolymerization Using Rh-Based Precatalysts: Resting State, Chain Control, and Efficient Polymer Synthesis

David E. Ryan, Kori A. Andrea, James J. Race, Timothy M. Boyd, Guy C. Lloyd-Jones, and Andrew S. Weller\*

Cite This: *ACS Catal.* 2020, 10, 7443–7448

Read Online

ACCESS |

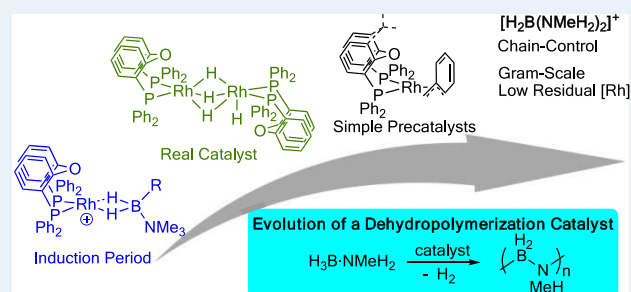
Metrics & More

Article Recommendations

Supporting Information

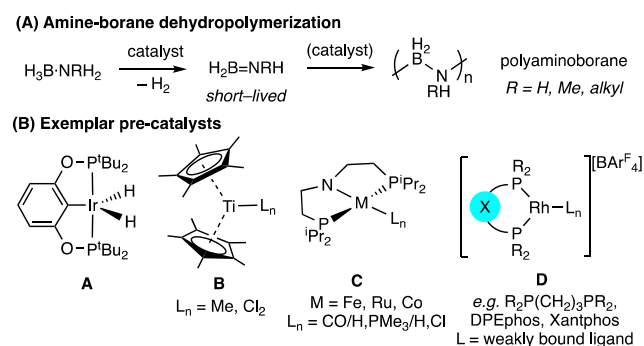
**ABSTRACT:** A detailed study of  $\text{H}_3\text{B}\cdot\text{NMeH}_2$  dehydropolymerization using the cationic precatalyst  $[\text{Rh}(\text{DPEphos})(\text{H}_2\text{BNMe}_3(\text{CH}_2)_2\text{Bu})][\text{BAR}^{\text{F}}_4]$  identifies the resting state as dimeric  $[\text{Rh}(\text{DPEphos})\text{H}_2]_2$  and boronium  $[\text{H}_2\text{B}(\text{NMeH}_2)_2]^+$  as the chain-control agent.  $[\text{Rh}(\text{DPEphos})\text{H}_2]_2$  can be generated in situ from  $\text{Rh}(\text{DPEphos})(\text{benzyl})$  and catalyzes polyaminoborane formation  $(\text{H}_2\text{BNMeH})_n$   $[M_n = 15\,000\text{ g mol}^{-1}]$ . Closely related  $\text{Rh}(\text{Xantphos})(\text{benzyl})$  operates at 0.1 mol % to give a higher molecular weight polymer  $[M_n = 85\,000\text{ g mol}^{-1}]$  on the gram scale with low residual  $[\text{Rh}]$ , 81 ppm. This insight offers a mechanistic template for dehydropolymerization.

**KEYWORDS:** dehydropolymerization, rhodium, phosphine, mechanism, amine–borane



The catalyzed dehydropolymerization of amine–boranes, archetypically  $\text{H}_3\text{B}\cdot\text{NMeH}_2$ , is an atom-efficient methodology for the synthesis of polyaminoboranes  $(\text{H}_2\text{BNRH})_n$  (Scheme 1A), forming  $\text{H}_2$  as the only byproduct.<sup>1–4</sup> This

## Scheme 1. (A) Amine–Borane Dehydropolymerization; (B) Exemplar Precatalyst Systems



new class of main-group polymer<sup>5</sup> is based upon BN main-chain units and is isosteric with technologically mature polyolefins. These main-chain B–N units suggest, in addition to unexplored material and chemical properties, potential applications as piezoelectric materials<sup>6,7</sup> or as precursors to boron-based ceramics and  $h\text{-BN}$ .<sup>1,8,9</sup>

The currently accepted overarching mechanism for polymer formation from amine–borane involves initial dehydrogen-

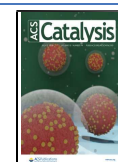
ation to form a transient<sup>10</sup> aminoborane ( $\text{H}_2\text{B}=\text{NRH}$ ) that then undergoes end-chain nucleophilic B–N bond formation initiated by the catalyst.<sup>3,11–16</sup> While noncatalytic routes have been reported,<sup>10,17</sup> in terms of overall efficiency, scalability, substrate scope, and control of the polymer characteristics, catalytic routes offer the broadest opportunity for the tailored synthesis of polyaminoboranes.

A wide range of precatalyst systems have been described for amine–borane dehydropolymerization (Scheme 1B). After the original report of high<sup>3</sup> molecular weight polymer formed using  $\text{Ir}(\text{POCOP})\text{H}_2$  **A** [ $\text{POCOP} = \kappa^3\text{-1,3-(}^t\text{Bu}_2\text{PO)}_2\text{C}_6\text{H}_3$ ],<sup>1,11</sup> systems based on group-4 metallocenes **B**,<sup>18,19</sup> cooperative ligands **C**,<sup>14,16,20,21</sup> and cationic  $[\text{RhL}_2]^+$  precatalysts ( $\text{L}_2 = \text{e.g., Ph}_2\text{P}(\text{CH}_2)_3\text{PPh}_2$ ,  $\text{DPEphos}$ ,  $\text{Xantphos}$ ) **D**<sup>22–24</sup> have been described. For the Rh-based catalysts, we have reported speciation, kinetics, and degree of polymerization studies. These are broadly generalized by an induction period, a nonliving chain-growth propagation, an inverse relationship between catalyst loading and degree of polymerization, and  $\text{H}_2$  acting as a chain controlling agent to reduce polymer chain length,<sup>15,22–24</sup> Scheme 2.

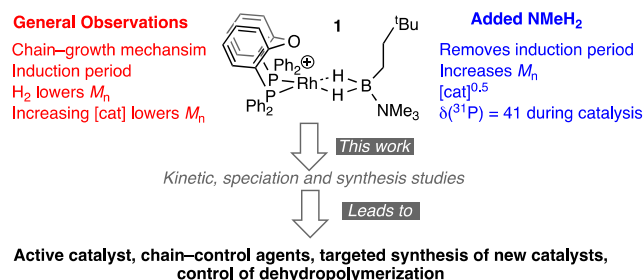
Received: May 19, 2020

Revised: June 15, 2020

Published: June 17, 2020



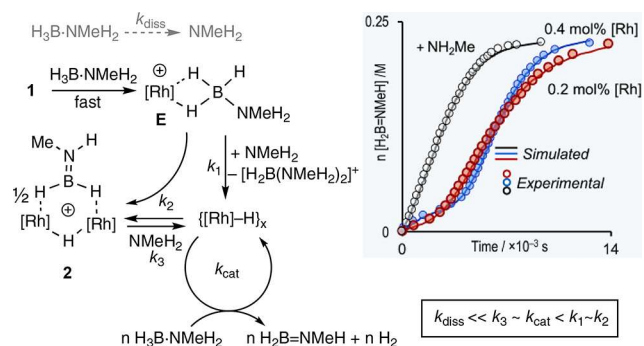
## Scheme 2. Exemplar Complex 1 and Prior Observations



We have also reported on the key role of NMeH<sub>2</sub>, formed by B–N bond cleavage in H<sub>3</sub>B·NMeH<sub>2</sub>,<sup>21,25</sup> Exemplified using the [Rh(DPEphos)(H<sub>2</sub>BNMe<sub>2</sub>CH<sub>2</sub>CH<sub>2</sub><sup>t</sup>Bu)][BAR<sup>F</sup><sub>4</sub>] precatalyst,<sup>23</sup> 1 [Ar<sup>F</sup> = 3,5-(CF<sub>3</sub>)<sub>2</sub>C<sub>6</sub>H<sub>3</sub>], the amine NMeH<sub>2</sub> removes the induction period, increases the degree of polymerization, and simplifies the kinetics, allowing a half order dependency on [Rh]<sub>TOTAL</sub> to be determined. However, the structure of the active catalyst is undetermined, with insight limited to the detection of a single species at  $\delta(^{31}P)$  41.3 [J(RhP) = 150 Hz]. Also lacking is a robust explanation for the relationship between [Rh]<sub>TOTAL</sub> and H<sub>2</sub> on the degree of polymerization.

Despite these advances, the precise details of initiation, propagation, and termination remain to be determined for these diverse catalyst systems,<sup>3</sup> while the identification of resting states is rare<sup>14,16</sup> and challenging.<sup>18</sup> Herein, we report on an investigation of the [Rh(DPEphos)]<sup>+</sup> precatalyst system, 1, in which a study of the kinetics, speciation, and synthesis has allowed the active catalyst to be identified, as well as the polymer-growth/termination processes to be interrogated. These insights are then harnessed in the design of a new, efficient, Rh-based catalyst that produces polyaminoborane on scale. A simple protocol is also described to significantly reduce the levels of residual catalyst in the isolated polymer.

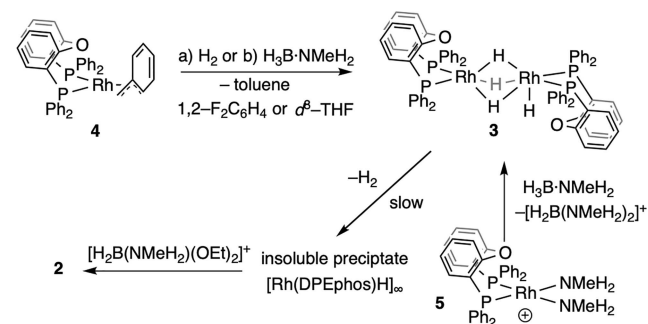
We have previously reported that, when 1 is employed as precatalyst, the monocationic hydrido-aminoborane dimer [Rh<sub>2</sub>(DPEphos)<sub>2</sub>(μ-H)(μ-H<sub>2</sub>B=NHMe)][BAR<sup>F</sup><sub>4</sub>] 2 is formed during the early stages of the reaction.<sup>23</sup> We propose this arises via an amine-promoted B–H hydride transfer<sup>26</sup> in a precursor cationic σ-amine–borane complex [Rh(DPEphos)(H<sub>3</sub>B·NMeH<sub>2</sub>)]<sup>+</sup>[BAR<sup>F</sup><sub>4</sub>]<sup>−</sup>, E,<sup>27</sup> to generate a neutral hydride of empirical formula Rh(DPEphos)H (Scheme 3). Similar hydride species are formed in [Rh(PONOP)(H<sub>3</sub>B·NMeH<sub>2</sub>)]<sup>+</sup><sup>25</sup> and [Rh(<sup>i</sup>Pr<sub>2</sub>P(CH<sub>2</sub>)<sub>3</sub>P<sup>i</sup>Pr<sub>2</sub>)(H<sub>3</sub>B·NH<sub>3</sub>)]<sup>+</sup><sup>28</sup> sys-

Scheme 3. Model and Fitted Data<sup>23 a</sup>

<sup>a</sup>[BAR<sup>F</sup><sub>4</sub>]<sup>−</sup> and DPEphos not shown. [H<sub>3</sub>B·NMeH<sub>2</sub>] = 0.223 M (1,2-F<sub>2</sub>C<sub>6</sub>H<sub>4</sub>).

tems, alongside H<sub>2</sub>B=NHMe<sub>2</sub>/[NMe<sub>2</sub>H<sub>2</sub>]<sup>+</sup> or boronium [H<sub>2</sub>B·(NH<sub>3</sub>)<sub>2</sub>]<sup>+</sup>, respectively. On the basis of these observations, a simple kinetics model was constructed for the induction process, involving generation of 2 by rapid trapping of Rh(DPEphos)H with unreacted E, followed by a slow, amine-dependent, fragmentation to form the active catalyst. This telescopes the elementary steps of the induction process,<sup>29</sup> allows H<sub>2</sub> evolution to be used as proxy for transient H<sub>2</sub>B=NHMeH, and successfully reproduces the temporal concentration profiles,<sup>23</sup> as a function of [Rh]<sub>TOTAL</sub> (0.2 and 0.4 mol %) or when NMeH<sub>2</sub> is added, Scheme 3. A VTNA analysis<sup>30,31</sup> supports the observation of an empirical fractional order in the precatalyst: [Rh]<sub>TOTAL</sub><sup>0.5</sup>.

With an effective model for the induction process determined, we then focused on identification of the catalyst resting state. On the basis of our model and the work of Fryzuk et al.<sup>32,33</sup> and Han and Tilley,<sup>34</sup> the neutral hydride bridged dimer [Rh(DPEphos)H]<sub>2</sub>, 3, was synthesized in situ by the addition of either H<sub>2</sub> or H<sub>3</sub>B·NMeH<sub>2</sub> to the new benzyl complex Rh(κ<sup>2</sup>-P,P-DPEphos)(η<sup>3</sup>-H<sub>2</sub>CPh) 4, Scheme 4.

Scheme 4. Synthesis and Reactivity of Complex 3<sup>a</sup>

<sup>a</sup>[BAR<sup>F</sup><sub>4</sub>]<sup>−</sup> not shown.

Toluene is formed in all cases. The 298 K <sup>31</sup>P{<sup>1</sup>H} NMR data for 3 match that observed during catalysis, i.e.,  $\delta$  41.3 [J(RhP) = 150 Hz, THF-*d*<sub>8</sub>]. The hydride ligands in 3 are fluxional at 298 K, presenting a very broad signal at  $\delta$  −8.1. Cooling to 253 K reveals three environments at  $\delta$  −6.9 (2H), −9.9 (1H), and −17.5 (1H). This pattern is similar to those reported for Rh<sub>2</sub>L<sub>4</sub>H<sub>4</sub> [L = P(O<sup>i</sup>Pr)<sub>3</sub>, 1/2 <sup>i</sup>Pr<sub>2</sub>P(CH<sub>2</sub>)<sub>3</sub>P<sup>i</sup>Pr<sub>2</sub>]<sup>32,35</sup> and is indicative of three bridging hydrides and one terminal hydride. The <sup>31</sup>P{<sup>1</sup>H} NMR spectrum of 3 at 253 K was poorly resolved, showing multiple, mutually coupled signals.

The addition of excess H<sub>3</sub>B·NMeH<sub>2</sub> to the amine complex [Rh(DPEphos)(NMeH<sub>2</sub>)<sub>2</sub>][BAR<sup>F</sup><sub>4</sub>], 5,<sup>23</sup> also generates 3, together with boronium [H<sub>2</sub>B(NMeH<sub>2</sub>)<sub>2</sub>]<sup>+</sup> [ $\delta(^{11}B)$  −7.8]. Solutions of complex 3 in 1,2-F<sub>2</sub>C<sub>6</sub>H<sub>4</sub>, or in THF, irreversibly lose H<sub>2</sub> on degassing to form an insoluble yellow/brown powder, analyzed as [Rh(DPEphos)H]<sub>∞</sub>, likely to be a coordination polymer with Rh–H–Rh linkages. While the Rh-polymer does not dissolve on the addition of H<sub>2</sub>, the soluble complex 2 is regenerated when [H<sub>2</sub>B(NMeH<sub>2</sub>)<sub>2</sub>](OEt<sub>2</sub>)]<sup>+</sup>[BAR<sup>F</sup><sub>4</sub>]<sup>−</sup> is added.<sup>10</sup> Thus, when using a cationic precatalyst (i.e., 1 or 5), persistent NMeH<sub>2</sub> will favor the soluble neutral hydride 3 via equilibration with complex 2 ( $k_3$ , Scheme 3). When using neutral precatalyst 4, a high initial concentration of amine–borane, e.g., [H<sub>3</sub>B·NMeH<sub>2</sub>]<sub>0</sub> = 0.446 M in THF, inhibits the formation of a precipitate. Presumably, the amine–borane intercepts Rh(DPEphos)H before it

oligomerizes. Thus, dimeric, neutral hydride **3** is observed as the common resting state, irrespective of the precatalyst or solvent. The half-order dependence in  $[\text{Rh}]_{\text{TOTAL}}$  points to a rapid endergonic equilibrium between dimer and monomer, prior to the turnover limiting step. This has been noted in other  $\text{Rh}_2\text{H}_x$  systems,<sup>32,36,37</sup> and the data are thus consistent with the resting state being dimeric **3**. An important difference between neutral versus cationic precatalysts is that the latter generate a boronium coproduct, which has important implications for the dehydropolymerization, as discussed next.

Neutral precatalyst **4** was deployed in the dehydropolymerization of  $\text{H}_3\text{B}\cdot\text{NMeH}_2$  at a variety of catalyst loadings, Table 1. Using 1,2- $\text{F}_2\text{C}_6\text{H}_4$  as the solvent, kinetics measurements

Table 1. GPC Characterization Data<sup>a</sup>

entry	cat.	$[\text{Rh}]_{\text{TOTAL}}$ (mol %)	$M_n$ [ $M_w$ ] (g mol <sup>-1</sup> ) <sup>b</sup>	$\bar{D}$	[boronium] (mol %)
1	4	0.25	15 000	2.5	0
2	4	0.5	15 000	2.5	0
3	4	1	15 000 [35 000]	2.4	0
4	4 <sup>c</sup>	0.5	17 000	2.3	0
5	4 <sup>c</sup>	1	17 000	2.4	0
6	4	1	[25 000]	n/a	0.25
7	4	1	[21 000]	n/a	0.5
8	4	1	[<19 000] <sup>d</sup>	n/a	1
9	6	1	88 000	1.5	0
10	6	1	21 000	1.5	1
11	6 <sup>c,e</sup>	0.1	85 000	1.5	0
13	7	1	98 000	1.6	0

<sup>a</sup>298 K, 1,2- $\text{F}_2\text{C}_6\text{H}_4$ , 0.223 M  $\text{H}_3\text{B}\cdot\text{NMeH}_2$ , isobaric conditions under a flow of Ar; end point determined by  $^{11}\text{B}$  NMR spectroscopy. <sup>b</sup>Relative to polystyrene standards; triple column; RI detection; THF with 0.1 w/w%  $[\text{NBu}_4]\text{Br}$ ; 35 °C; [sample] = 2 mg cm<sup>-3</sup>. <sup>c</sup>THF solvent. <sup>d</sup> $M_p$  of the polymer distribution obscured by the  $[\text{BAR}^{\text{F}}_4]^-$  signal. <sup>e</sup>5 M, 1.1 g scale.

were hampered by the formation of the insoluble precipitate. In THF, eudiometric measurements on  $\text{H}_2$  production were less reliable due to solvent volatility. Nevertheless, polymerization goes to completion in both solvents, selectively forming  $[\text{H}_2\text{BNMeH}]_n$  (Figure 1A).<sup>38</sup> A plot of conversion versus  $M_n$  (Figure 1B, relative to polystyrene standards)<sup>3,11,16</sup> is characteristic of a nonliving chain-growth polymerization: at low conversions, the polymer is formed with high  $M_n$  and  $\text{H}_3\text{B}\cdot\text{NMeH}_2$  dominates. Variations in catalyst loading did not affect the degree of polymerization of the resulting polyaminoborane, in either 1,2- $\text{F}_2\text{C}_6\text{H}_4$  (Figure 1C,  $M_n$  = 15 000 g mol<sup>-1</sup>) or THF solutions ( $M_n$  = 17 000 g mol<sup>-1</sup>), under “open conditions” with a slow Ar flow. This is different from cationic precatalysts, such as **1**, where  $M_n$  scales inversely with  $[\text{Rh}]_{\text{TOTAL}}$ : e.g., 6400 (1 mol %) and 34 900 g mol<sup>-1</sup> (0.2 mol %).<sup>23</sup> However, “closed conditions” that allow for buildup of  $\text{H}_2$  result in very low molecular weight oligomers being formed (1 mol % **4**, less than 1000 g mol<sup>-1</sup> by GPC,  $^{11}\text{B}$  NMR spectroscopy<sup>31</sup>). The cationic precatalyst **1** behaves analogously.<sup>22</sup>

The neutral and cationic precatalyst systems differ by the presence of a boronium coproduct with the latter, the relative concentration of which will scale with  $[\text{Rh}]_{\text{TOTAL}}$ .<sup>39</sup> Given the underlying insensitivity to the degree of polymerization to  $[\text{Rh}]_{\text{TOTAL}}$  when using neutral **4**, we thus considered whether with cationic precatalysts boronium  $[\text{H}_2\text{B}(\text{NMeH}_2)_2][\text{BAR}^{\text{F}}_4]$  can act as a chain-control agent to modify  $M_n$ . To test this,

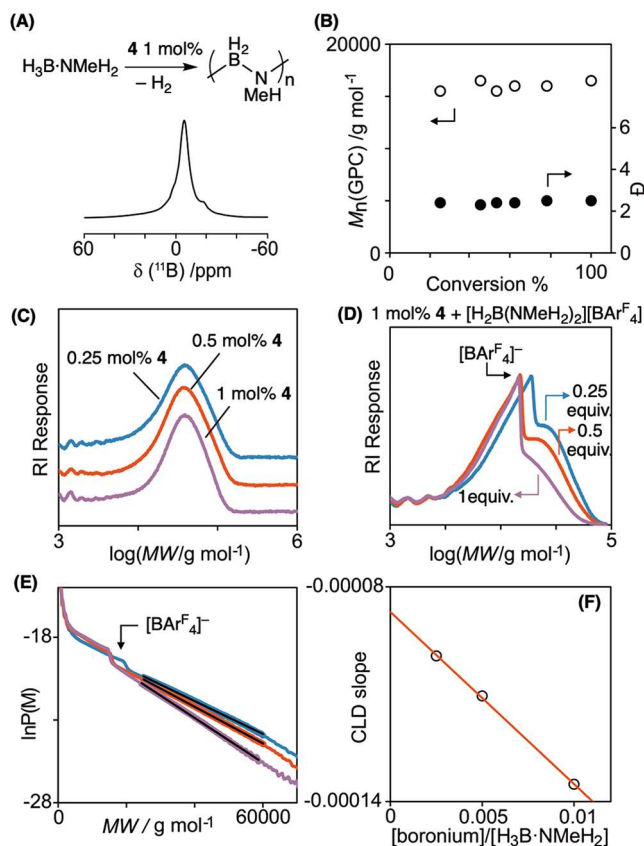


Figure 1. Polyaminoborane data obtained using catalyst **4** (Ar flow, 1,2- $\text{F}_2\text{C}_6\text{H}_4$ ,  $\text{H}_3\text{B}\cdot\text{NMeH}_2$  = 0.223 M). (A)  $^{11}\text{B}$  NMR spectrum of the polymer; (B)  $M_n$  versus conversion; (C) GPC data for 1.0, 0.5, and 0.25 mol % catalyst loadings; (D) GPC data for 1.0 mol % **4** with  $[\text{H}_2\text{B}(\text{NMeH}_2)_2][\text{BAR}^{\text{F}}_4]$  doping; (E)  $\ln$ -CLD plot of the high  $M_w$  fraction (D); (F) Mayo analysis.

$[\text{H}_2\text{B}(\text{NMeH}_2)_2][\text{BAR}^{\text{F}}_4]$  was doped (0.25 to 1 mol %) into 1 mol % **4**/ $\text{H}_3\text{B}\cdot\text{NMeH}_2$  to selectively form polyaminoborane ( $^{11}\text{B}$  NMR). Although GPC analysis of the resulting polymer using refractive index detection is affected by the coeluting  $[\text{BAR}^{\text{F}}_4]^-$  masking the lower molecular weight region (Figure 1D),<sup>15</sup> there is a qualitative trend of decreasing  $M_p$  with increasing  $[\text{H}_2\text{B}(\text{NMeH}_2)_2][\text{BAR}^{\text{F}}_4]$ , Table 1. This outcome is consistent with boronium acting as a chain-control agent. Chain length distribution ( $\ln$ -CLD) analysis of high molecular weight fractions in GPC has been shown to be useful where there is overlap between distributions of polymer and transfer agents, such as that noted here, allowing for chain control processes to be probed.<sup>40</sup> A Mayo-type plot of  $[\text{boronium}]/[\text{H}_3\text{B}\cdot\text{NMeH}_2]$  versus the  $\ln$ -CLD slope indicates an inversely linear relationship (Figure 1E,F), further supporting the conclusion that the boronium functions as a rapid chain control agent in the dehydropolymerization.

Collectively, the analysis above facilitates the construction of a mechanistic landscape for dehydropolymerization, Scheme 5, that is consistent not only with the results herein but also with our previous observations on cationic Rh-based systems.<sup>15,22,23,28,41</sup> Thus, dehydrogenation of amine-borane to give the reactive monomer,  $\text{H}_2\text{B}=\text{NMeH}$ , occurs at a neutral  $[\text{Rh}-\text{H}]$  species in an  $\text{H}_2$ -mediated equilibrium with dimer **3**. Dehydrogenation to form  $\text{H}_2\text{B}=\text{NMeH}$  via BH/NH activation (Scheme 5A) could be facilitated by a hemilabile DPEphos ligand (e.g.,  $\kappa^2$  and  $\kappa^3$  coordination<sup>42</sup>) as previously





**Kori A. Andrea** – Department of Chemistry, Memorial University of Newfoundland, St. John's, Newfoundland A1B 3X7, Canada

**James J. Race** – Department of Chemistry, University of York, York YO10 SDD, United Kingdom; Department of Chemistry, Chemical Research Laboratories, University of Oxford, Oxford OX1 3TA, United Kingdom; [orcid.org/0000-0002-2134-3796](https://orcid.org/0000-0002-2134-3796)

**Timothy M. Boyd** – Department of Chemistry, University of York, York YO10 SDD, United Kingdom; Department of Chemistry, Chemical Research Laboratories, University of Oxford, Oxford OX1 3TA, United Kingdom; [orcid.org/0000-0001-6607-3761](https://orcid.org/0000-0001-6607-3761)

**Guy C. Lloyd-Jones** – School of Chemistry, University of Edinburgh, Edinburgh EH9 3FJ, United Kingdom; [orcid.org/0000-0003-2128-6864](https://orcid.org/0000-0003-2128-6864)

Complete contact information is available at:  
<https://pubs.acs.org/10.1021/acscatal.0c02211>

### Author Contributions

The manuscript was written through contributions of all authors.

### Notes

The authors declare no competing financial interest.

### ACKNOWLEDGMENTS

The authors acknowledge Drs. Romaeo Dallanegra and Adrian Chaplin for the synthesis and characterization of  $[\text{Rh}(\kappa^2\text{-P,P-DPEphos})(\eta^2\eta^2\text{-H}_3\text{B-NMe}_3)][\text{BAR}^{\text{F}}_4]$  and Dr. Antonio Martinez-Martinez for useful discussions. EPSRC EP/M024210, the NSERC Vanier Canada Graduate Scholarship, and Michael Smith Foreign Study Supplement (KAA) are also acknowledged.

### REFERENCES

- (1) Staubitz, A.; Presa Soto, A.; Manners, I. Iridium-Catalyzed Dehydrocoupling of Primary Amine–Borane Adducts: A Route to High Molecular Weight Polyaminoboranes, Boron–Nitrogen Analogues of Polyolefins. *Angew. Chem., Int. Ed.* **2008**, *47*, 6212–6215.
- (2) Leitao, E. M.; Jurca, T.; Manners, I. Catalysis in service of main group chemistry offers a versatile approach to p-block molecules and materials. *Nat. Chem.* **2013**, *5*, 817–829.
- (3) Colebatch, A. L.; Weller, A. S. Amine–Borane Dehydropolymerization: Challenges and Opportunities. *Chem. - Eur. J.* **2019**, *25*, 1379–1390.
- (4) Han, D.; Anke, F.; Trose, M.; Beweries, T. Recent advances in transition metal catalyzed dehydropolymerisation of amine boranes and phosphine boranes. *Coord. Chem. Rev.* **2019**, *380*, 260–286.
- (5) Vidal, F.; Jäkle, F. Functional Polymeric Materials Based on Main-Group Elements. *Angew. Chem., Int. Ed.* **2019**, *58*, 5846–5870.
- (6) Nakhmanson, S. M.; Nardelli, M. B.; Bernholc, J. Ab Initio Studies of Polarization and Piezoelectricity in Vinylidene Fluoride and BN-Based Polymers. *Phys. Rev. Lett.* **2004**, *92*, 115504.
- (7) Zhang, Y.; Hopkins, M. A.; Liptrot, D. J.; Khanbarez, H.; Groen, P.; Zhou, X.; Zhang, D.; Bao, Y.; Zhou, K.; Bowen, C. R.; Carbery, D. R. Harnessing Plasticity in an Amine–Borane as a Piezoelectric and Pyroelectric Flexible Film. *Angew. Chem., Int. Ed.* **2020**, *59*, 7808–7812.
- (8) Du, V. A.; Jurca, T.; Whittell, G. R.; Manners, I. Aluminum borate nanowires from the pyrolysis of polyaminoborane precursors. *Dalton Trans.* **2016**, *45*, 1055–1062.
- (9) Wang, X.; Hooper, T. N.; Kumar, A.; Priest, I. K.; Sheng, Y.; Samuels, T. O. M.; Wang, S.; Robertson, A. W.; Pacios, M.; Bhaskaran, H.; Weller, A. S.; Warner, J. H. Oligomeric aminoborane precursors for the chemical vapour deposition growth of few-layer hexagonal boron nitride. *CrystEngComm* **2017**, *19*, 285–294.
- (10) Metters, O. J.; Chapman, A. M.; Robertson, A. P. M.; Woodall, C. H.; Gates, P. J.; Wass, D. F.; Manners, I. Generation of aminoborane monomers  $\text{RR}'\text{N-BH}_2$  from amine–boronium cations  $[\text{RR}'\text{N}^+\text{H-BH}_2\text{L}]^+$ : metal catalyst-free formation of polyaminoboranes at ambient temperature. *Chem. Commun.* **2014**, *50*, 12146–12149.
- (11) Staubitz, A.; Sloan, M. E.; Robertson, A. P. M.; Friedrich, A.; Schneider, S.; Gates, P. J.; Schmedt auf der Gönne, J.; Manners, I. Catalytic Dehydrocoupling/Dehydrogenation of N-Methylamine–Borane and Ammonia–Borane: Synthesis and Characterization of High Molecular Weight Polyaminoboranes. *J. Am. Chem. Soc.* **2010**, *132*, 13332–13345.
- (12) Baker, R. T.; Gordon, J. C.; Hamilton, C. W.; Henson, N. J.; Lin, P.-H.; Maguire, S.; Murugesu, M.; Scott, B. L.; Smythe, N. C. Iron Complex-Catalyzed Ammonia–Borane Dehydrogenation. A Potential Route toward B–N-Containing Polymer Motifs Using Earth-Abundant Metal Catalysts. *J. Am. Chem. Soc.* **2012**, *134*, 5598–5609.
- (13) Bhunya, S.; Malakar, T.; Paul, A. Unfolding the crucial role of a nucleophile in Ziegler–Natta type Ir catalyzed polyaminoborane formation. *Chem. Commun.* **2014**, *50*, 5919–5922.
- (14) Glüer, A.; Förster, M.; Celinski, V. R.; Schmedt auf der Gönne, J.; Holthausen, M. C.; Schneider, S. Highly Active Iron Catalyst for Ammonia Borane Dehydrocoupling at Room Temperature. *ACS Catal.* **2015**, *5*, 7214–7217.
- (15) Adams, G. M.; Colebatch, A. L.; Skornia, J. T.; McKay, A. I.; Johnson, H. C.; Lloyd-Jones, G. C.; Macgregor, S. A.; Beattie, N. A.; Weller, A. S. Dehydropolymerization of  $\text{H}_3\text{B-NMeH}_2$  To Form Polyaminoboranes Using  $[\text{Rh}(\text{Xantphos-alkyl})]$  Catalysts. *J. Am. Chem. Soc.* **2018**, *140*, 1481–1495.
- (16) Anke, F.; Boye, S.; Spannenberg, A.; Lederer, A.; Heller, D.; Beweries, T. Dehydropolymerisation of methylamine borane and an N-substituted primary amine borane using a PNP Fe catalyst. *Chem. - Eur. J.* **2020**, *26*, 7889–7899.
- (17) De Albuquerque Pinheiro, C. A.; Roiland, C.; Jehan, P.; Alcaraz, G. Solventless and Metal-Free Synthesis of High-Molecular-Mass Polyaminoboranes from Diisopropylaminoborane and Primary Amines. *Angew. Chem., Int. Ed.* **2018**, *57*, 1519–1522.
- (18) LaPierre, E. A.; Patrick, B. O.; Manners, I. Trivalent Titanocene Alkyls and Hydrides as Well-Defined, Highly Active, and Broad Scope Precatalysts for Dehydropolymerization of Amine–Boranes. *J. Am. Chem. Soc.* **2019**, *141*, 20009–20015.
- (19) Jurca, T.; Dellermann, T.; Stubbs, N. E.; Resendiz-Lara, D. A.; Whittell, G. R.; Manners, I. Step-growth titanium-catalysed dehydropolymerisation of amine–boranes. *Chem. Sci.* **2018**, *9*, 3360–3366.
- (20) Knitsch, R.; Han, D.; Anke, F.; Ibing, L.; Jiao, H.; Hansen, M. R.; Beweries, T. Fe(II) Hydride Complexes for the Homogeneous Dehydrocoupling of Hydrazine Borane: Catalytic Mechanism via DFT Calculations and Detailed Spectroscopic Characterization. *Organometallics* **2019**, *38*, 2714–2723.
- (21) Boyd, T. M.; Andrea, K. A.; Baston, K.; Johnson, A.; Ryan, D. E.; Weller, A. S. A simple cobalt-based catalyst system for the controlled dehydropolymerisation of  $\text{H}_3\text{B-NMeH}_2$  on the gram-scale. *Chem. Commun.* **2020**, *56*, 482–485.
- (22) Johnson, H. C.; Leitao, E. M.; Whittell, G. R.; Manners, I.; Lloyd-Jones, G. C.; Weller, A. S. Mechanistic Studies of the Dehydrocoupling and Dehydropolymerization of Amine–Boranes Using a  $[\text{Rh}(\text{Xantphos})]^+$  Catalyst. *J. Am. Chem. Soc.* **2014**, *136*, 9078–9093.
- (23) Adams, G. M.; Ryan, D. E.; Beattie, N. A.; McKay, A. I.; Lloyd-Jones, G. C.; Weller, A. S. Dehydropolymerization of  $\text{H}_3\text{B-NMeH}_2$  Using a  $[\text{Rh}(\text{DPEphos})]^+$  Catalyst: The Promoting Effect of  $\text{NMeH}_2$ . *ACS Catal.* **2019**, *9*, 3657–3666.
- (24) Colebatch, A. L.; Hawkey Gilder, B. W.; Whittell, G. R.; Oldroyd, N. L.; Manners, I.; Weller, A. S. A General, Rhodium-Catalyzed, Synthesis of Deuterated Boranes and N-Methyl Polyaminoboranes. *Chem. - Eur. J.* **2018**, *24*, 5450–5455.

- (25) Spearing-Ewyn, E. A. K.; Beattie, N. A.; Colebatch, A. L.; Martinez-Martinez, A. J.; Docker, A.; Boyd, T. M.; Baillie, G.; Reed, R.; Macgregor, S. A.; Weller, A. S. The role of neutral Rh(PONOP)H, free NMe<sub>2</sub>H, boronium and ammonium salts in the dehydrocoupling of dimethylamine-borane using the cationic pincer [Rh(PONOP)( $\eta^2$ -H<sub>2</sub>)]<sup>+</sup> catalyst. *Dalton Trans.* **2019**, 48, 14724–14736.
- (26) Roselló-Merino, M.; López-Serrano, J.; Conejero, S. Dehydrocoupling Reactions of Dimethylamine-Borane by Pt(II) Complexes: A New Mechanism Involving Deprotonation of Boronium Cations. *J. Am. Chem. Soc.* **2013**, 135, 10910–10913.
- (27) See the [Supporting Information](#) for the model complex for E: [Rh( $\kappa^2$ -P,P-DPEphos)( $\eta^2$ -H<sub>3</sub>B-NMe<sub>3</sub>)] [BAr<sup>F</sup><sub>4</sub>].
- (28) Kumar, A.; Beattie, N. A.; Pike, S. D.; Macgregor, S. A.; Weller, A. S. The Simplest Amino-borane H<sub>2</sub>B = NH<sub>2</sub> Trapped on a Rhodium Dimer: Pre-Catalysts for Amine–Borane Dehydropolymerization. *Angew. Chem., Int. Ed.* **2016**, 55, 6651–6656.
- (29) These will be defined and discussed in a future contribution.
- (30) Nielsen, C. D. T.; Burés, J. Visual kinetic analysis. *Chem. Sci.* **2019**, 10, 348–353.
- (31) See the [Supporting Information](#).
- (32) Fryzuk, M. D.; Piers, W. E.; Einstein, F. W. B.; Jones, T. Coordinatively unsaturated binuclear clusters of rhodium. The reactivity of [{Pr<sup>i</sup><sub>2</sub>P(CH<sub>2</sub>)<sub>n</sub>PPr<sup>i</sup><sub>2</sub>}Rh]<sub>2</sub>( $\mu$ -H)<sub>2</sub> (n = 2, 3, and 4) with dihydrogen, and their use in the catalytic hydrogenation of olefins. *Can. J. Chem.* **1989**, 67, 883–896.
- (33) Fryzuk, M. D.; McConville, D. H.; Rettig, S. J. Synthesis, structure and hydrogenation of  $\eta^3$ -benzyl diphosphine complexes of rhodium and iridium. *J. Organomet. Chem.* **1993**, 445, 245–256.
- (34) Han, L.-B.; Tilley, T. D. Selective Homo- and Heterodehydrocouplings of Phosphines Catalyzed by Rhodium Phosphido Complexes. *J. Am. Chem. Soc.* **2006**, 128, 13698–13699.
- (35) Sivak, A. J.; Muetterties, E. L. Metal clusters. 21. Synthesis of rhodium phosphite clusters. *J. Am. Chem. Soc.* **1979**, 101, 4878–4887.
- (36) Kumar, A.; Ishibashi, J. S. A.; Hooper, T. N.; Mikulas, T. C.; Dixon, D. A.; Liu, S.-Y.; Weller, A. S. The Synthesis, Characterization and Dehydrogenation of Sigma-Complexes of BN-Cyclohexanes. *Chem. - Eur. J.* **2016**, 22, 310–322.
- (37) Brown, J. M.; Lloyd-Jones, G. C. Vinylborane Formation in Rhodium-Catalyzed Hydroboration of Vinylarenes. Mechanism versus Borane Structure and Relationship to Silation. *J. Am. Chem. Soc.* **1994**, 116, 866–878.
- (38) Monitoring by NMR spectroscopy (1 mol %, THF, closed system) shows no induction period.
- (39) Some neutral precatalyst systems may also produce coproducts that scale with [cat], such as boronium or ammonium, through amine-promoted M–Cl for M–H metathesis. See ref 21.
- (40) Moad, G.; Moad, C. L. Use of Chain Length Distributions in Determining Chain Transfer Constants and Termination Mechanisms. *Macromolecules* **1996**, 29, 7727–7733.
- (41) Dallanegra, R.; Robertson, A. P. M.; Chaplin, A. B.; Manners, I.; Weller, A. S. *Chem. Commun.* **2011**, 47, 3763.
- (42) Adams, G. M.; Weller, A. S. POP-type ligands: Variable coordination and hemilabile behaviour. *Coord. Chem. Rev.* **2018**, 355, 150–172.
- (43) Esteruelas, M. A.; Nolis, P.; Oliván, M.; Oñate, E.; Vallribera, A.; Vélez, A. Ammonia Borane Dehydrogenation Promoted by a Pincer-Square-Planar Rhodium(I) Monohydride: A Stepwise Hydrogen Transfer from the Substrate to the Catalyst. *Inorg. Chem.* **2016**, 55, 7176–7181.
- (44) Addy, D. A.; Bates, J. I.; Kelly, M. J.; Riddlestone, I. M.; Aldridge, S. Aminoborane  $\sigma$  Complexes: Significance of Hydride Coligands in Dynamic Processes and Dehydrogenative Borylene Formation. *Organometallics* **2013**, 32, 1583–1586.
- (45) Chain-capping events have been discussed in phosphine–borane dehydropolymerization. Oldroyd, N. L.; Chitnis, S. S.; Annibale, V. T.; Arz, M. I.; Sparkes, H. A.; Manners, I. Metal-free dehydropolymerisation of phosphine-boranes using cyclic (alkyl)(amino)carbenes as hydrogen acceptors. *Nat. Commun.* **2019**, 10, 1370.
- (46) Turner, J. R.; Resendiz-Lara, D. A.; Jurca, T.; Schäfer, A.; Vance, J. R.; Beckett, L.; Whittell, G. R.; Musgrave, R. A.; Sparkes, H. A.; Manners, I. Synthesis, Characterization, and Properties of Poly(aryl)phosphinoboranes Formed via Iron-Catalyzed Dehydropolymerization. *Macromol. Chem. Phys.* **2017**, 218, 1700120.

#### ■ NOTE ADDED AFTER ASAP PUBLICATION

This paper was originally published ASAP on June 24, 2020, with an error in Scheme 4. The corrected version was reposted on June 29, 2020.